NANO LETTERS

Letter

Stacking-Faults-Free Zinc Blende GaAs Nanowires

Hadas Shtrikman, Ronit Popovitz-Biro, Andrey Kretinin, and Moty Heiblum

Nano Lett., **2009**, 9 (1), 215-219• DOI: 10.1021/nl8027872 • Publication Date (Web): 18 December 2008

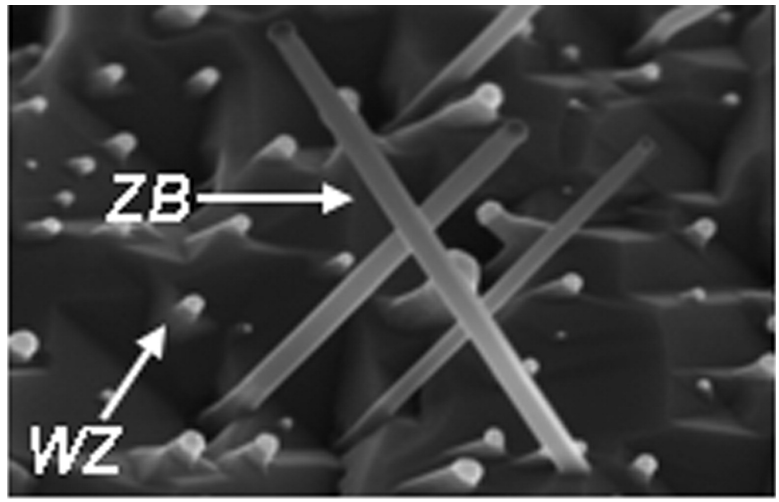

More About This Article

Additional resources and features associated with this article are available within the HTML version:

- Supporting Information
- Access to high resolution figures
- Links to articles and content related to this article
- Copyright permission to reproduce figures and/or text from this article

View the Full Text HTML

NANO LETTERS

2009
Vol. 9, No. 1
215-219

Stacking-Faults-Free Zinc Blende GaAs Nanowires

Hadas Shtrikman,*,† Ronit Popovitz-Biro,‡ Andrey Kretinin,† and Moty Heiblum†

Braun Center for Submicron Research and Electron Microscopy Unit, Weizmann Institute of Science, Rehovot, Israel

Received September 14, 2008; Revised Manuscript Received November 20, 2008

ABSTRACT

Stacking-faults-free zinc blende GaAs nanowires have been grown by molecular beam epitaxy using the vapor−liquid−solid gold assisted growth method. Two different approaches were used to obtain continuous low supersaturation in the vicinity of the growing wires. A double distribution of gold droplets on the (111)B surface in the first case, and a highly terraced (311)B growth surface in the second case both avoided the commonly observed transition to wurtzite structure.

One-dimensional nanowires made of III−V compound semiconductors attract increasing interest for their use in studying fundamental physics problems[1−5] as well as for potential applications.[6−9] In general, semiconductor nanowires are nucleated and grown via the vapor−liquid−solid (VLS) mechanism with the assistance of metal droplets (gold droplets are commonly used).[10−13] Nanowire diameters and lengths are determined by the size of the gold droplets and the growth duration, respectively; however, their shape is strongly determined by growth conditions such as group V/III flux ratio and substrate temperature. The VLS method enables growth of semiconductor nanowires with large aspect ratio while producing an extremely uniform diameter along the entire wire length, making them unique 1D conducting channels, waveguides, or nanosize electromechanical systems (NEMS). Presently, the ability to control the quality of nanowires in terms of their microstructure is still a challenging task regardless of the growth method used, be it MOCVD,[10,12,14,15] CBE,[16] or MBE.[13,17−20] Here we report on growth of nanowires by the MBE method.

The quality of III−V nanowires, and in particular GaAs nanowires, had already been the subject of numerous papers facing the problem of the hexagonal wurtzite (WZ) structure dominating the microscopic structure of such wires.[21−23] This is in contrast to bulk or two-dimensional epitaxial growth which are cubic having the zinc blende (ZB) structure. The current understanding is that beyond a critically small diameter which lies in the range of 10−30 nm the free energies of the WZ and ZB structures become comparable,[22,24] resulting in occasional stacking faults forming between alternating layers of WZ and ZB along the ⟨111⟩ axis of the nanowires. In turn, stacking faults are considered to be deleterious to carrier transport, such as ballistic transport, and luminescence. Unfortunately, the overlap region between both polytypes happens to be of most importance for the common nanowire applications.

GaAs wires having ZB structure were identified branching from WZ wires grown on a (011) GaAs surface.[20] Samuelson et al. managed to grow ZB InP and InAs/InP wires by avoiding melting of the substrate beneath the gold droplets.[16,25] While the growth of ZB nanowires was addressed on a few occasions,[18,26] the growth of pure ZB GaAs nanowires by MBE has not yet been reported. The possibility of growing pure ZB nanowires had already been suggested by Hiruma et al.[10] They speculated that lowering the growth temperature of GaAs nanowires would favor ZB stacking; however, as it turned out, by lowering the growth temperature sufficiently, the wires had multiple stacking faults embedding relatively large regions of ZB in between. Moreover, growth at low temperature induced strong tapering along the wires, rendering them useless. Here we demonstrate the growth and characterization of stacking-faults-free ZB GaAs nanowires, via the VLS method adapted to our MBE system.

In order to impose suitable conditions under which ZB stacking would persist, it is instructive to list the conditions under which GaAs preferably assumes the ZB structure. First and foremost is the bulk form of GaAs which is always ZB (unless external pressure is applied[27]). Second, during the initiation of growth, and before the wires change their stacking to WZ, they emerge from the bulk in ZB form.[21] Third, at the tip of the nanowire, in the vicinity of the interface between the wire and the gold droplet (initiated by closing the Ga source), a change to ZB stacking is commonly observed. A characteristic example of such transition for a GaAs nanowire grown in the ⟨0001⟩ direction can be seen

* To whom correspondence should be addressed. E-mail: hadas.shtrikman@weizmann.ac.il.
† Braun Center for Submicron Research.
‡ Electron Microscopy Unit.

10.1021/nl8027872 CCC: $40.75
Published on Web 12/18/2008

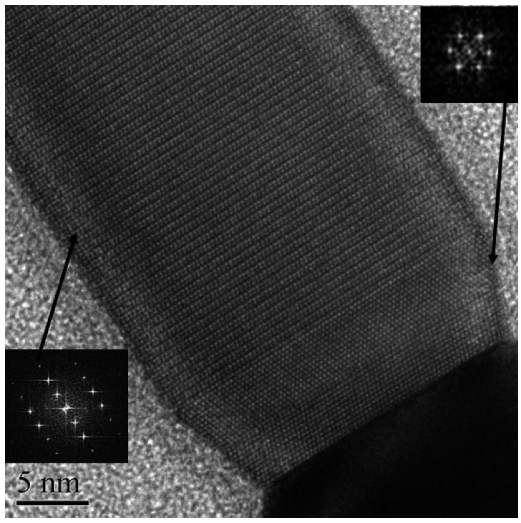

Figure 1. TEM micrograph of a WZ GaAs nanowire growing in the ⟨0001⟩ direction. Structural transition from WZ to ZB near the interface with the gold is clearly seen. The Fourier transforms of the WZ and ZB sections are on the left- and right-hand side of the image, respectively.

in Figure 1. Glas et al.[21] has related the above ubiquitous observations to low supersaturation conditions during the growth of these phases. Intuitively, one would think that lowering of the Ga impinging rate or increasing of group V/III ratio would result in the appropriate condition of low supersaturation. However, from our experiments reducing the Ga arrival rate merely reduces the length of the nanowires maintaining a WZ structure. Similarly, when the group V/III ratio is increased, suppression of the growth of WZ GaAs wires results in no ZB wires emerging.

On the basis of these observations we aimed at developing a procedure of growth under continuous low supersaturation conditions. We chose two different routes to impose low supersaturation growth conditions. The first, by applying a particularly thick layer of gold (1.5−2 nm) on a (111)B surface of GaAs, which upon melting above the eutectic temperature formed a double-size distribution of gold droplets. A high density of large gold droplets (100−200 nm diameter) is formed among a lower density of smaller gold droplets (30−50 nm diameter). Ga atoms that impinged on the surface were more likely to be absorbed by one of the large gold droplets, leading to strong competition over Ga atoms by the small gold droplets. Similarly, a second approach was to use the highly terraced (311)B surface, which is composed of a high density of short terraces. Atoms impinging on the terraces were very likely to be trapped at the step edges before managing to reach the gold droplets. Both procedures were expected to lead to a lower saturation in the vicinity of the gold droplets which developed into long wires.

GaAs nanowires were grown by MBE (in a Riber 32 solid source system) using the VLS method. A layer of gold was evaporated directly on the GaAs substrate, after an initial oxide removal (in a separate chamber attached to the MBE system) by heating the substrate to 600 °C. For growth on (111)B or on the (311)B substrate, a gold layer 1.5−2 nm

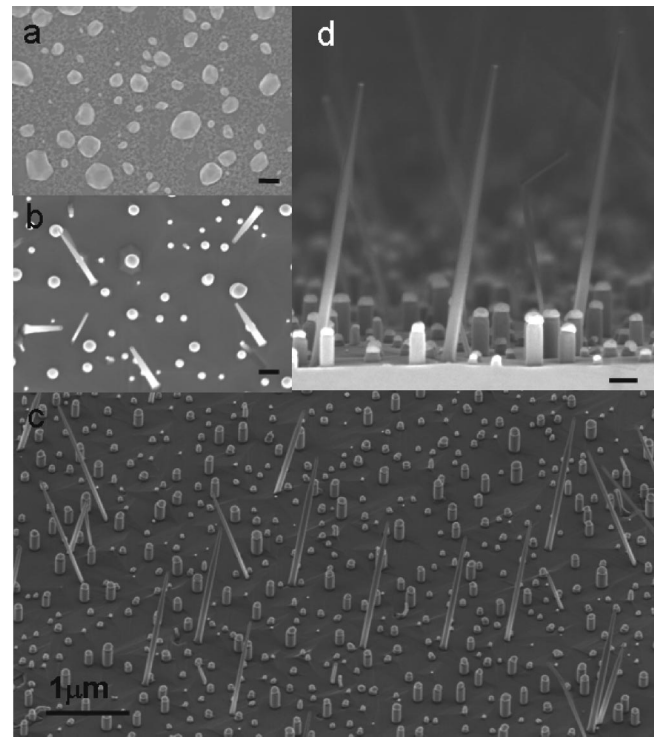

Figure 2. SEM images: (a) top view of a pregrowth double distribution of gold droplets (scale bar 200 nm); (b) top view (scale bar 200 nm), (c) 45° view, and (d) side view of GaAs nanowires grown on a (111)B surface with a double size distribution of gold droplets (scale bar 200 nm).

or ∼0.5 nm thick, respectively, was evaporated. Note that the thinner gold layer was shown to produce a uniform distribution of droplets on a (111)B surface under similar conditions of heat treatment. Subsequently, the wafer was moved into the attached MBE growth chamber where GaAs nanowire growth was initiated at a substrate temperature of 600 °C and an As_4/Ga flux ratio on the order of 200. The growth temperature used for growth on both substrates, (111)B and (311)B, was chosen to be relatively high (50 °C higher than our standard growth temperature for WZ wires), in order to further reduce the supersaturation also by enhancement of the bulk growth.

The analysis of the morphological and structural properties of the wires was performed by scanning electron microscopy (SEM) (Zeiss Supra 55 system at 2 kV) and transmission electron microscopy (TEM) (for normal resolution, a Philips CM120 microscope operating at 120 kV; for high resolution, a Tecnai F30 UT operating at 300 kV). Samples examined by TEM were prepared by dispersing nanowires in ethanol using an ultrasonic bath for 1 min, followed by spreading a drop from the suspension on a 300 mesh carbon/collodion/Cu or lacy carbon/Cu grid.

Figure 2a shows a SEM image of the pregrowth distribution of gold droplets on the (111)B GaAs surface where the double diameters distribution is evident. The top view (Figure 2b) shows the distribution of as-grown wires, which is comparable to the original gold droplets distribution. Figure 2c, taken at 45°, clearly shows the general distribution of the tilted thin and long wires among the short ones that are

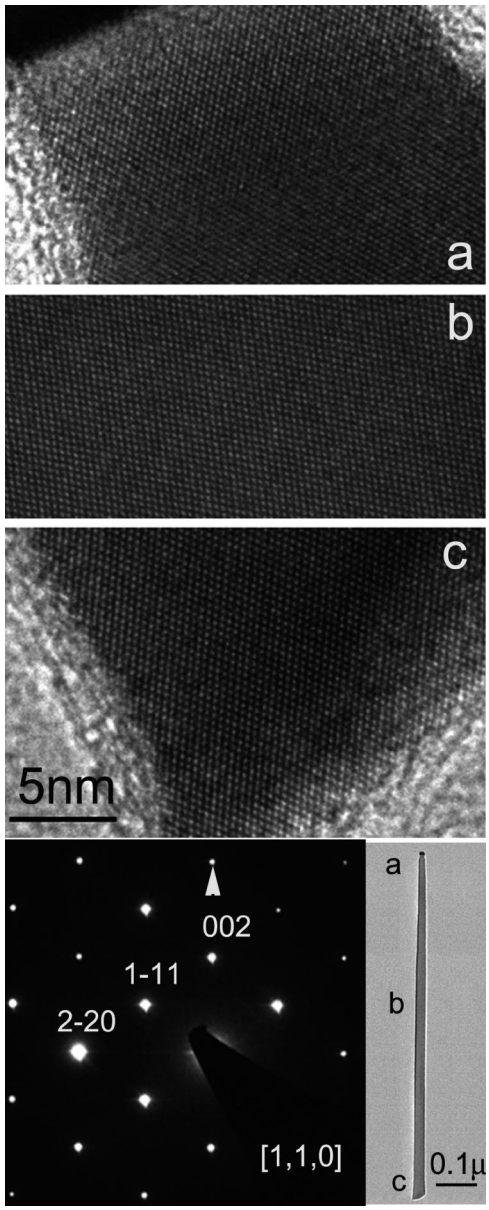

Figure 3. (a−c) HRTEM images taken from the top, center, and bottom of a ZB GaAs nanowire grown on a (111)B surface as marked in the low-magnification TEM image (bottom right). Bottom left is the electron diffraction from the center of the wire; the arrow indicates the growth direction of the wire.

perpendicular to the substrate. The large diameter wires grew perpendicularly to the surface and are relatively short (∼200 nm long) and actually cover up a significant part of the surface, whereas the smaller diameter wires are much longer and are tilted with respect to the substrate by some ∼80° (either in the ⟨001⟩ or in the ⟨011⟩ direction).

Systematic inspection by TEM of the thin, long nanowires revealed a perfect ZB crystal structure, free of stacking faults. A TEM micrograph of a typical wire is seen in Figure 3. Most tips of the ZB wires have one or more diagonal twin planes symmetrically situated on both sides. This is similar to the tips of WZ wires that grow in the ⟨0001⟩ direction (Figure 1). In the WZ case, the twin plane is exactly perpendicular to the ⟨0001⟩ growth direction. However, in the ZB wires, since the ⟨111⟩ axis is no longer aligned

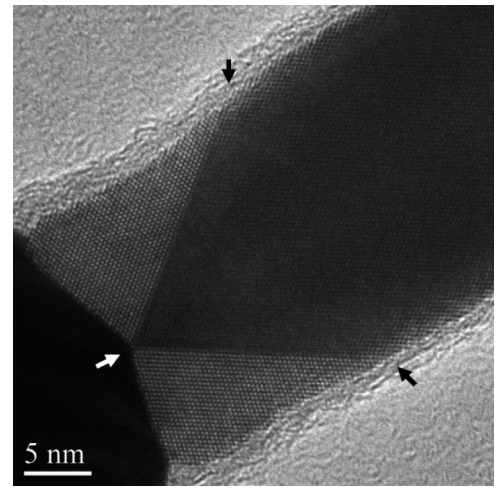

Figure 4. TEM image of a ZB GaAs nanowire exhibiting two converging diagonal twin planes, emerging from the perimeter into a single spot (the arrows are guides to the eye).

perpendicularly to the growth front, the twin planes form an angle of 36° with the growth direction. These twin planes emerge from the wire edge propagating inward, which means that they nucleate at the wire perimeter. This serves as a unique demonstration of the growth mechanism at the gold droplet/nanowire interface, showing that nucleation indeed occurs at the *triple phase boundary* (between gold, nanowire, and vacuum).[21,28] While occasionally only a single twin plane was observed on either side of the wire, we also found wires with both twin planes merging into a single point inside the wire (see Figure 4).

Now we relate to the other method that minimizes supersaturation, namely, growth on (311)B. The (311)B surface is formed by tilting the (100) surface by 25° toward the (111)B surface; hence it is a highly terraced vicinal surface with typically ∼6 Å wide terraces. Atoms impinging on such small terraces are quickly absorbed by the step ledges as well as at the kinks along the terraces. The thickness of the evaporated gold layer was ∼0.5 nm, only a third of that used to form the double distribution on the (111)B substrates. Note that this thickness assured uniform size distribution of gold droplets after annealing on a (111)B surface. Figure 5a shows a strikingly uniform distribution of long, tilted, pure ZB wires, which grew among a dense population of very short, undeveloped, WZ wires in between. The tilt angle of the long wires is some ∼70° to the surface (Figure 5d). This angle happens to be similar to the angle between the [311] and the [001] directions which is 72.4°. However, a more detailed understanding of the tilt angle of the ZB wires growing on both the (111)B and the (311)B surfaces requires further study including a better statistical survey.

Indeed, TEM micrographs once again proved that the crystalline structure of the long wires is a pure, completely free of stacking faults, ZB crystal lattice (see Figure 6a, b, and c). In a similar fashion to ZB wires grown on the (111)B surface, the majority of the wires grew in the ⟨001⟩ direction, having four {110} facets, while others grew in the {110} direction having two {011} and two {001} facets. In Figure 6d a typical electron diffraction pattern of a nanowire, which

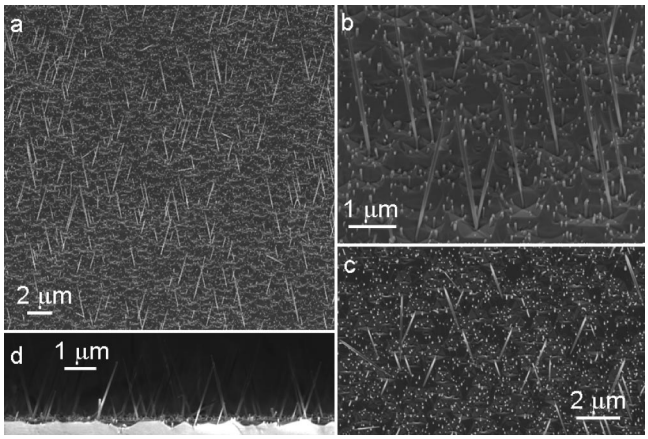

Figure 5. SEM images of GaAs nanowires grown on a (311)B surface: (a, b) 45° views at different magnifications; (c) top view; (d) side view.

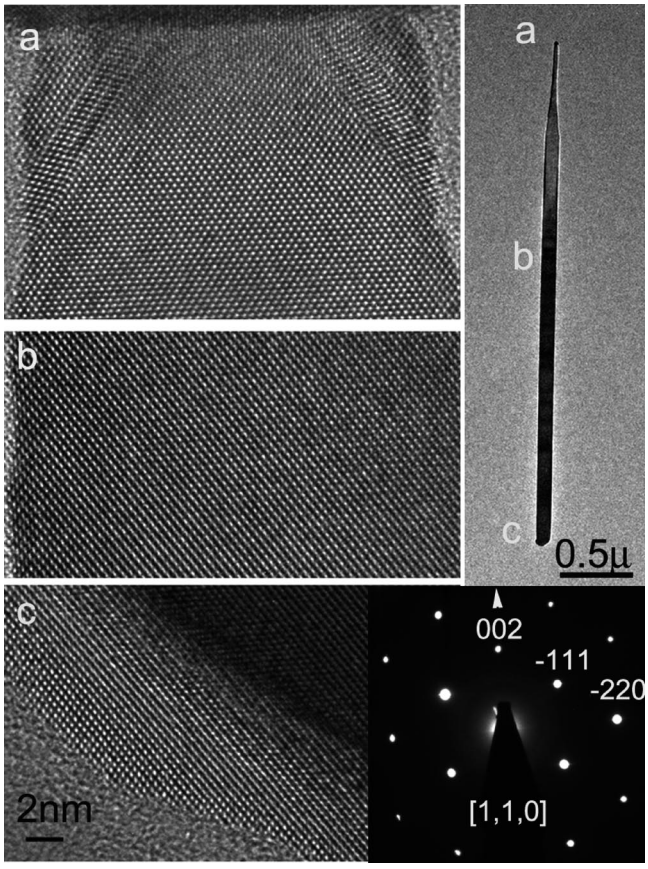

Figure 6. (a−c) HRTEM images taken from the top, center, and bottom of a ZB GaAs nanowire grown on a (311)B surface as marked in the low-magnification TEM of the wire (top right). Bottom right is the electron diffraction from the center of the wire; the arrow indicates the growth direction of the wire.

is viewed from the [110] direction, displays the growth orientation of the nanowire-being in this case ⟨001⟩.

We looked at fully grown ZB wires with well-developed side facets. Growth of such side facets takes place via a two-dimensional growth mechanism of atoms that impinge on the surface of the substrate and climb up to the gold droplet and others that directly impinge on the side walls (possibly due to the tilt angle with respect to the impinging supply of

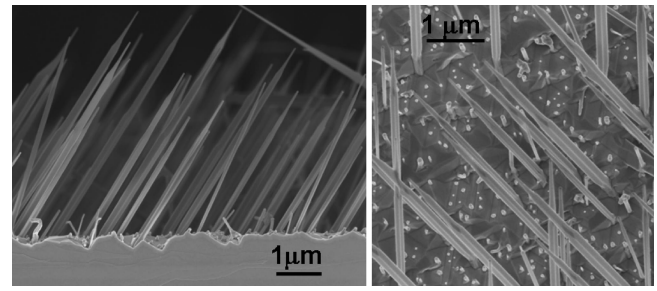

Figure 7. SEM side view (left) and top view (right) of ZB GaAs nanowires grown on a (311)B surface.

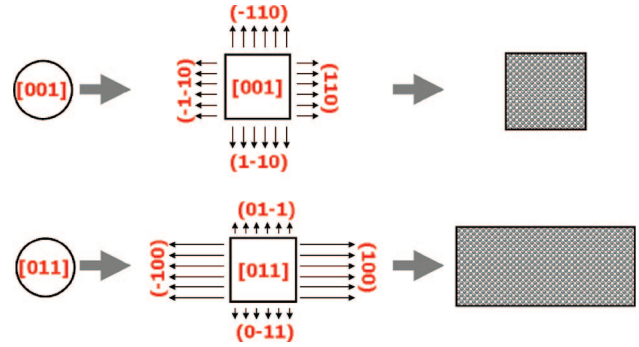

Figure 8. Schematic top view of ZB GaAs nanowires growing in the [001] (top) and [011] (bottom) directions; {001} and {011} are fast and slow growing planes, respectively.

atoms).[17] Figure 7 is a SEM image of the as-grown ZB wires, which discloses the fact that the ZB nanowires can grow in two distinct shapes, one having a square cross section and the other a rectangular one. Systematic TEM studies of such wires further suggested that both shapes are related to growth in the ⟨001⟩ and ⟨011⟩ growth directions, respectively. As noted above, among the analyzed wires the majority grew in the ⟨001⟩ direction. In the initial stage of growth the cross section of all wires was circular and their diameter was determined by that of the gold droplet. The wires growing in the ⟨001⟩ direction gradually develop four identical {110} side facets, which grow at the same rate, thus forming a square cross section. However, the wires that grew in the ⟨011⟩ direction had two opposite {011} type facets and two opposite {100} type facets. Due to their inert nature the {011} facets are very slow growing ones compared to the {100} facets, leading to a rectangular cross section.[16,25,29] Both processes are schematically illustrated in Figure 8. The growth rate of different types of facets was used before to explain the morphology of GaP−GaAs nanowires.[30]

It is noteworthy that under such low supersaturation conditions the wires nucleating as ZB are unlikely to form stacking faults since once formed, as in the case of bulk growth, their energy is lower than that of the WZ, and thus there would be no driving force for the structural transformation.

A noticeable advantage of growth on the (311)B surface, which systematically produces wires having the ZB structure, is the fact that part of the surface is covered by short WZ nanowires, ensuring a lower density of the ZB nanowires and a spread-out distribution thereof. Sufficient scarcity

eliminates interaction between nearby wires and is more conducive for external coating in processes such as the formation of core/shell structures. This approach is clearly more advantageous than the commonly used procedure of passivating the surface between the wires by spinning of polylysine[15] which is incompatible with any ultrahigh purity processes.

In conclusion, we showed that the growth of pure GaAs ZB wires by MBE using the VLS method is feasible and can produce stacking-fault-free nanowires. This can be achieved by locally reducing supersaturation conditions, thus preventing a transition to a WZ stacking, as we demonstrated using two different approaches: high concentration of large diameter gold droplets on the (111)B surface, consuming excess elemental deposits in the first case; and growth on the (311)B surface, having numerous surface steps, which also capture the supplied atoms, in the second case. Both methods provided competition over the impinging atoms, allowing for smaller droplets in between to evolve into fully grown ZB nanowires.

Acknowledgment. The transmission electron microscopy studies were conducted at the Irving and Cherna Moskowitz Center for Nano and Bio-Nano Imaging at the Weizmann Institute of Science. The authors acknowledge Perla Kacman for illuminating discussions on the structure of III−V nanowires. H.S. is grateful to Lars Samuelson for his initial guidance and to Ray LaPierre and Martin Plante for very fruitful discussions. Thanks to Meirav Dolev for an enlightening conversation.

References

(1) Doh, Y. J.; van Dam, J. A.; Roest, A. L.; Bakkers, E. M. P. A.; Kouwenhoven, L. P.; De Franceschi, S. Tunable supercurrent through semiconductor nanowires. *Science* **2005**, *309*, 272.
(2) Xiang, J.; Vidan, A.; Tinkham, M.; Westervelt, R. M.; Lieber, C. M. Ge/Si nanowire mesoscopic Josephson junctions. *Nat. Nanotechnol.* **2006**, *1*, 208.
(3) Fasth, C.; Fuhrer, A.; Samuelson, L.; Golovach, V. N.; Loss, D. Direct measurement of the spin−orbit interaction in a two-electron InAs nanowire quantum dot. *Phys. Rev. Lett.* **2007**, *98*, 266801.
(4) Sand-Jespersen, T.; Paaske, J.; Andersen, B. M.; Grove-Rasmussen, K.; Jorgensen, H. I.; AAgesen, M.; Sorensen, C. B.; Lindelof, P. E.; Flensberg, K.; Nygard, J. Kondo-enhanced Andreev tunneling in InAs nanowires quantum dots. *Phys. Rev. Lett.* **2007**, *99*, 126603.
(5) Fuhrer, A.; Fasth, C.; Samuelson, L. Single electron pumping in InAs nanowire double quantum dots. *Appl. Phys. Lett.* **2007**, *91*, 52109.
(6) Lu, W.; Lieber, C. M. Nanoelectronics from the bottom up. *Nat. Mater.* **2007**, *6*, 841.
(7) Minot, E. D.; Kelkensberg, F.; van Kouwen, M.; van Dam, J. A.; Kouwenhoven, L. P.; Zwiller, V.; Borgström, M. T.; Wunnicke, O.; Verheijen, M. A.; Bakkers, E. P. A. M. Single quantum dot nanowire LEDs. *Nano Lett.* **2007**, *7*, 367.
(8) Qian, F.; Gradecak, S.; Li, Y.; Wen, C. Y.; Lieber, C. M. Core/Multishell Nanowire Heterostructures as Multicolor, High-Efficiency Light-Emitting Diodes. *Nano Lett.* **2005**, *5*, 2287.
(9) Lu, W.; Lieber, C. M. Semiconductor nanowires. *J. Phys. D: Appl. Phys.* **2006**, *39*, R387.
(10) Hiruma, K.; Yazawa, M.; Haraguchi, K.; Ogawa, K.; Katsuyama, T.; Koguchi, M.; Kakibayashi, H. GaAs free-standing quantum-size wires. *J. Appl. Phys.* **1993**, *74*, 3162.
(11) Duan, X.; Lieber, C. M. General synthesis of compound semiconductor nanowires. *Adv. Mater.* **2000**, *12*, 298.
(12) Ohlsson, B. J.; Bjork, M. T.; Magnusson, M. H.; Deppert, K.; Samuelson, L.; Wallenberg, L. R. Size-, shape-, and position-controlled GaAs nano-whiskers. *Appl. Phys. Lett.* **2001**, *79*, 3335.
(13) Tchernycheva, M.; Harmand, J. C.; Patriarche, G.; Travers, L.; Cirlin, G. E. Temperature conditions for GaAs nanowire formation by Au-assisted molecular beam epitaxy. *Nanotechnology* **2006**, *17*, 4025.
(14) Joyce, H. J.; Gao, Q.; Tan, H. H.; Jagadish, C.; Kim, Y.; Zhang, X.; Guo, Y.; Zou, J. Twin-free uniform epitaxial GaAs nanowires grown by a two-temperature process. *Nano Lett.* **2007**, *7*, 921.
(15) Wacaser, B. A.; Deppert, K.; Karlsson, L. S.; Samuelson, L.; Seifert, W. Growth and characterization of defect free GaAs nanowires. *J. Cryst. Growth* **2006**, *287*, 504.
(16) Bojrk, M. T.; Ohlsson, B. J.; Sass, T.; Persson, A. I.; Thelander, C.; Magnusson, M. H.; Deppert, K.; Wallenberg, L. R.; Samuelson, L. One-dimensional heterostructures in semiconductor nanowhiskers. *Appl. Phys. Lett.* **2002**, *6*, 1058.
(17) Chen, C.; Plante, M. C.; Fradin, C.; LaPierre, R. R. Layer-by-layer and step-flow growth mechanisms in GaAsP/GaP nanowire heterostructures. *J. Mater. Res.* **2006**, *21*, 2801. Plante, M. C.; LaPierre, R. R. Au-assisted growth of GaAs nanowires by gas source molecular beam epitaxy: tapering, sidewall faceting and crystal structure. *J. Cryst. Growth* **2008**, *310*, 356.
(18) Dheeraj, D. L.; Patriarche, G.; Largear, L.; Zhou, H. L.; van Helvoort, A. T.; Glas, F.; Harmand, J. C.; Fimland, B. O.; Weman, H. Zinc blende GaAsSb nanowires grown by molecular beam epitaxy. *Nanotechnology* **2008**, *19*, 1.
(19) Mariager, S. O.; Sørensen, C. B.; Aagesen, M.; Nygård, J.; Feidenhans'l, R.; Willmott, P. R. Facet structure of GaAs nanowires grown by molecular beam epitaxy. *Appl. Phys. Lett.* **2007**, *91*, 83106.
(20) Wu, Z. H.; Mei, X.; Kim, D.; Blumin, M.; Ruda, H. E.; Liu, J. Q.; Kavanagh, K. L. Growth, branching, and kinking of molecular-beam epitaxial 0.110. GaAs nanowires. *Appl. Phys. Lett.* **2003**, *83*, 3368.
(21) Glas, F.; Harmand, J. C.; Patriarche, G. Why does wurtzite form in nanowires of III-V zinc blende semiconductors. *Phys. Rev. Lett.* **2007**, *99*, 146101.
(22) Galicka, M.; Bukala, M.; Buczko, R.; Kacman, P. Modelling the structure of GaAs and InAs Nanowires. *J. Phys.: Condens. Matter* **2008**, *20*, 454226.
(23) Dubrovskii, V. G.; Sibirev, N. V. Growth thermodynamics of nanowires and its application to polytypism of zinc blende III-V nanowires. *Phys. Rev. B* **2008**, *77*, 035414.
(24) Akiyama, T.; Sano, K.; Nakamura, K., III. *Appl. Phys.* **2006**, *45*, L275.
(25) Krishnamachari, U.; Borgstrom, M.; Ohlsson, B. J.; Panev, N.; Samuelson, L.; Seifert, W.; Larsson, M. W.; Wallenberg, L. R. Defect-free nanowires grown in [001] direction on InP (001). *Appl. Phys. Lett.* **2004**, *85*, 2077.
(26) Johansson, J.; Karlsson, L. S.; Svensson, C. P. T.; Martensson, T.; Wacaser, B. A.; Deppert, K.; Samuelson, L.; Seifert, W. Structural properties of κB-oriented III-V nanowires. *Nat. Mater.* **2006**, *5*, 574. Zhang, X. T.; Liu, Z.; Leung, Y. P.; Li, Q.; Hark, S. K. Growth and luminescence of zinc-blende-structured ZnSe nanowires by metal-organic chemical vapor deposition. *Appl. Phys. Lett.* **2003**, *83*, 5533. Chi, Y.; Chan, C. S.; Sou, I. K.; Chan, Y. F.; Su, D. S.; Wang, N. The size-dependent growth direction of ZnSe nanowires. *Adv. Mater.* **2006**, *18*, 109.
(27) Wang, S. Q.; Ye, H. Q. A plane-wave pseudopotential study on III-V zinc-blende and wurtzite semiconductors under pressure. *J. Phys.: Condens. Matter* **2002**, *14*, 9579.
(28) Wacaser, B. A. *Doctoral dissertation: Nanoscale Crystal Growth - The importance of Interfaces and Phase Boundaries*. Lund University, 2007.
(29) Verheijen, M. A.; Algra, R. E.; Borgstrom, M. T.; Immink, G.; Sourty, E.; van Enckevort, W. J. P.; Vlieg, E.; Bakkers, E. P. A. M. Three-dimensional morphology of GaP-GaAs nanowires revealed by transmission electron microscopy tomography. *Nano Lett.* **2007**, *7*, 3051.
(30) Verheijen, M. A.; Algra, R. E.; Borgstrom, M. T.; Immink, G.; Soury, E.; van Enckevort, W. J. P.; Vlieg, E.; Bakkers, E. P. A. M. Three-dimensional morphology of GaP-GaAs nanowires revealed by transmission electron microscopy tomography. *Nano Lett.* **2007**, *7*, 3051.

NL8027872